Ashdin Publishing
Journal of Advanced Chemical Engineering
Vol. 1 (2011), Article ID A110602, 11 pages
doi:10.4303/jace/A110602

Research Article

Microfluidic Reactor for Sequential Operation of Polymerase Chain Reaction/Ligase Detection Reaction

Masahiko Hashimoto,[1] Kazuhiko Tsukagoshi,[1] and Steven A. Soper[2]

[1]*Department of Chemical Engineering and Materials Science, Faculty of Science and Engineering, Doshisha University, 1-3 Miyakodani, Tatara, Kyotanabe-Shi, Kyoto 610-0321, Japan*
[2]*Department of Chemistry, Center for Bio-Modular Multi-Scale Systems, Louisiana State University, Baton Rouge, LA 70803, USA*
Address correspondence to Masahiko Hashimoto, mahashim@mail.doshisha.ac.jp

Received 21 June 2011; Revised 28 August 2011; Accepted 2 September 2011

Abstract We have developed a microfluidic bioreactor for detecting single base mutations in genomic DNA, where a primary polymerase chain reaction (PCR) and an allele-specific ligation detection reaction (LDR) were conducted in sequence. The effect of carryover from the primary PCR on the subsequent LDR was thoroughly investigated in terms of LDR yield and fidelity, and we found that a post-PCR treatment for the amplicons prior to its incorporation into the LDR phase was not necessarily required, which allowed us to use a simple diffusive mixer to online mix the post-PCR solution with the LDR reagents. We also performed a numerical analysis to roughly estimate a channel length required for the diffusive mixing. We successfully demonstrated the ability of the system to detect one mutant DNA in 1000 normal sequences at a relatively high processing speed (total processing time = ca. 28.1 min).

Keywords polymerase chain reaction; ligase detection reaction; microfluidic bioreactor; DNA point mutation; continuous-flow; enzymatic reaction

1 Introduction

One major issue towards DNA mutation detection in practical samples such as tissue biopsy samples or circulating DNA is that the mutation of interest (mutant DNA) may be present in a mixed population of higher copy numbers of wild-type DNA. Therefore, high sensitivity technologies are required to capture mutant signals in the presence of a vast majority of normal DNA. Direct sequencing has the advantage of identifying the location and the nature of a mutation simultaneously, however current sequencing techniques are not applicable for cancer detection because of their low sensitivity. Allele-specific amplification techniques are prone to false positive signals from minute contamination or from the introduction of point mutations by polymerase errors during PCR amplification.

One technique that can distinguish low-abundant mutant DNA from wild-type DNA is the ligase detection reaction (LDR) coupled to a primary polymerase chain reaction (PCR) [2,4,5,6,10,17,18,27,30]. A conceptual scheme of the PCR-coupled LDR technique is depicted in Figure 1. Following PCR amplification of the appropriate gene fragments, which contain sections of the gene(s) that possess the point mutations, the amplicon is mixed with two LDR primers (common primer and discriminating primer) that flank the mutation of interest at an appropriate temperature. The discriminating primer contains a base at its $3'$-end that coincides with the single base mutation site. If there is a mismatch, ligation of the two primers does not essentially occur. However, a perfect match results in a successful ligation of the two primers and produces a product that can be analyzed in a variety of fashions such as polyacrylamide gel electrophoresis [2,17,18] and microarrays [4,5,6,10, 27,30]. The advantages of PCR/LDR are that it can be configured to do highly multiplexed assays and uses a thermally stable enzyme to linearly amplify the LDR product.

Recently, attention has focused on developing microfluidic reactor for biological amplifications that require temperature cycling, such as PCR [3,9,16,19,20,21,25], dideoxy cycle sequencing [26,29], ligase chain reaction (LCR) [22] and ligase detection reaction (LDR) [7,8, 10] since they can offer a lower thermal capacitance, require smaller amounts of reagents for the reaction, possess the potential for automation, and can be integrated to subsequent processing steps configured on chips to minimize sample contamination, which is extremely important to circumvent in clinical settings for early detection of a disease. During the past decade, a number of groups have designed chamber-type PCR chips, where a stationary PCR mixture in a confined space is alternatively heated and cooled [3,16,19,21]. Alternatively, DNA amplification can be achieved in a microfluidic platform by shuttling a PCR cocktail in a microchannel repetitively through different isothermal zones using a continuous-flow (CF) format [7,8,9,20,25]. The CFPCR approach can be

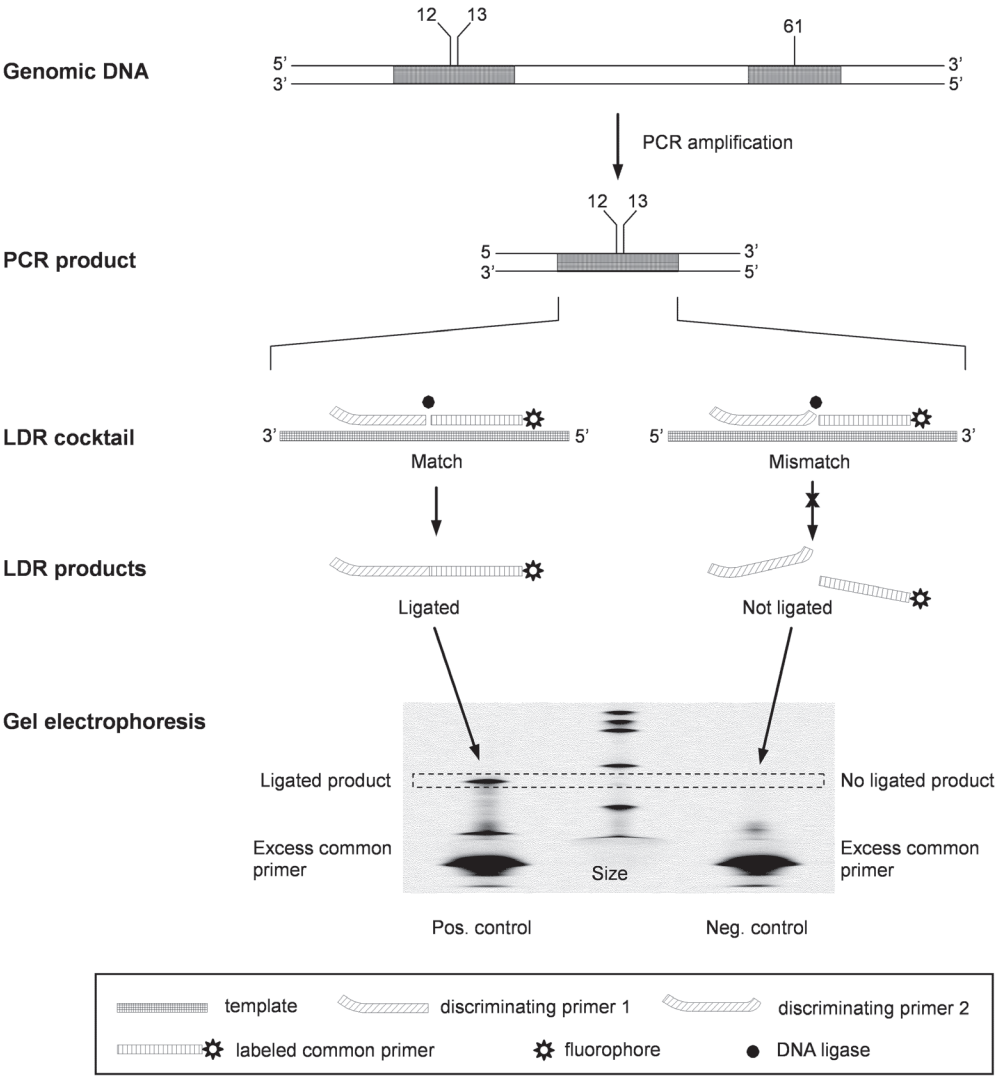

Figure 1: Conceptual schematic of the PCR/LDR assay. First, the DNA strand containing the single base-pair difference (wild-type or mutant) is PCR amplified. The PCR-amplified DNA is then used in LDR. In the LDR phase, the thermostable ligase will only ligate primers that are perfectly complementary to their target sequence, resulting in fluorescence signal of the ligation products at an appropriate position in a gel matrix (as shown in the left branch). Primers that have at least a single base-pair mismatch at the $3'$-end contributing to the junction of the two primers will not ligate, producing no fluorescence signature (as shown in the right branch).

conducted at relatively high speeds since it is not necessary to heat and cool the large thermal mass associated with the amplification chamber repeatedly.

In the previous paper, we reported on the development of a polymer-based flow-through biochip, where a primary PCR process and subsequent LDR were integrated onto a single chip incorporating thermal cycling units [8]. Both PCR process and subsequent LDR were sequentially operated in a CF format, which allowed for rapid product generation for the detection of low-abundant mutations directly from an input of a small amount of genomic DNA. We employed Stoffel fragment, which lacked $5'\rightarrow3'$ exonuclease activity, or the conventional *Taq*, which possessed $5'\rightarrow3'$ exonuclease activity, as a DNA polymerase in the primary PCR phase and briefly investigated how they affected a serially-coupled secondary reaction and how reagent selection could produce optimal results for coupled sequential biological reactions using PCR/LDR as an example. We revealed that the incorporation of those polymerases into the LDR phase did not interfere with producing the targeted LDR products but generated different artifacts.

In this work, we slightly modified the previous microchannel design to render a four-times larger thermal

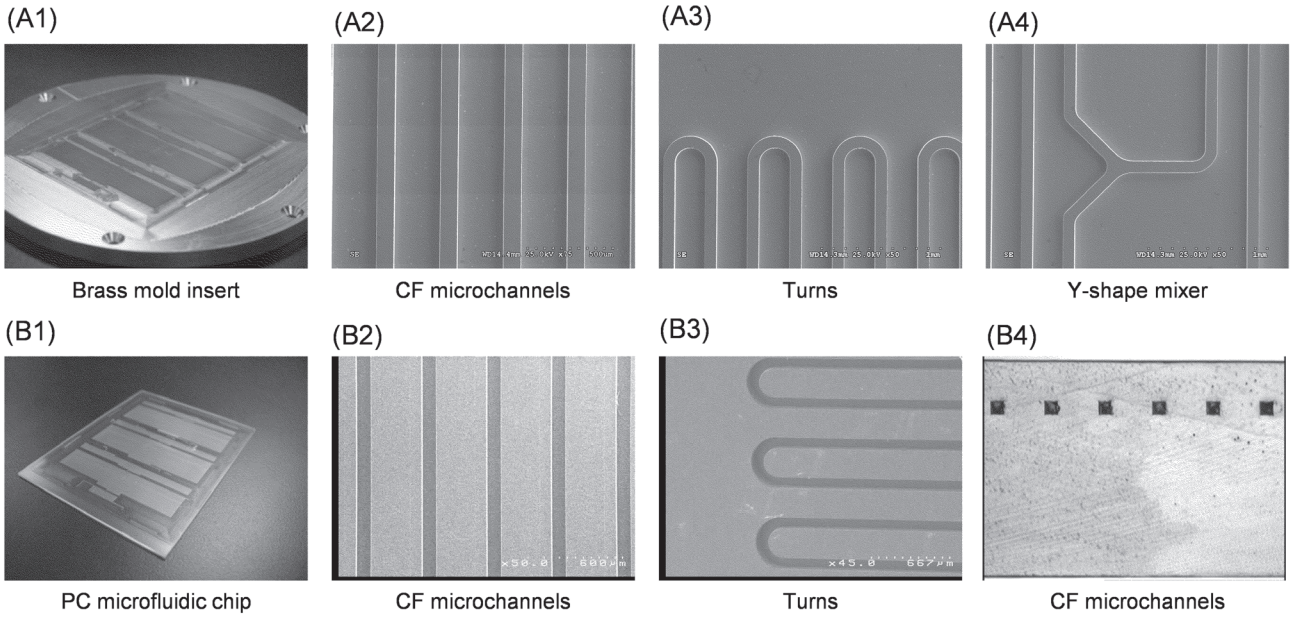

Figure 2: Images for the brass mold insert (A1)–(A4) and PC replicate (B1)–(B4). The images for A2, A3, A4, B2 and B3 were captured by a scanning electron microscope. For, B4, the PC chip sealed by a cover plate was smoothly cut perpendicular to the multiple channels and the cross-sectional image was taken by a microscope equipped with a CCD camera.

cycling number (40 cycles) to the exponential amplification nature of PCR process than to the linear amplification nature of LDR process for enhancing the targeted LDR product output. We chose Stoffel fragment as a DNA polymerase, which was revealed in the previous study to provide larger PCR product amounts and less artifacts in the secondary LDR step than the conventional *Taq*. Then, we thoroughly investigated how the artifacts were exactly generated from an input of a small amount of genomic DNA in the course of the sequential PCR/LDR amplifications using both the microfluidic reactors and a commercial thermal cycler. We also performed a numerical analysis to roughly estimate a channel length required for diffusive mixing of the PCR product solution with the LDR cocktail between the first- and the second-round amplifications.

2 Experimental

2.1 Chip fabrication

A mold master for the CFPCR/CFLDR microfluidic reactor was fabricated in brass (353 engravers' brass, McMaster-Carr, Atlanta, GA) using a high-precision micromilling machine (Kern MMP 2522; Kern Micro-und Feinwerktechnik GmbH, Marnau, Germany) ((A1)–(A4) in Figure 2). Micromilling was carried out at 40000 rpm using 1000, 200 and 50 μm-diameter milling bits (McMaster-Carr). A typical milling cycle consisted of precuting the entire surface with the 1000 μm milling bit to ensure parallelism between both faces of the brass plate to guarantee a uniform height of the milled microstructures over the entire pattern, rough milling of the microstructures using the 200 μm diameter milling bit, and finishing with a 50 μm bit. The thermal cycling channel was 2.02 m and 0.50 m long for CFPCR and CFLDR, respectively, which allowed for 40-cycles for PCR and 10-cycles for LDR. This channel was 100 μm in width, 100 μm in depth and possessed a 250 μm inter-channel spacing.

Replicates from the brass dies were hot-embossed into PC substrates (McMaster-Carr, Atlanta, GA) ((B1)–(B4) in Figure 2). The embossing system consisted of a PHI Precision Press model number TS-21-H-C (4A)-5 (City of Industry, CA). A vacuum chamber was installed into this press to remove air (pressure $<$ 0.1 bar) to minimize replication errors. During embossing, the molding die for the CFPCR/CFLDR microchannel was heated to 190 °C and pressed into the PC wafer with a force of 850 lb for 5 min. After hot embossing, the press was opened and the polymer part removed and cooled to room temperature.

Sealing of the PC microchannel with a cover plate was critical due to the elaborate pattern of the microchannel topography and the high glass transition temperature of PC. The embossed substrate (1 mm thick) and the top cover plate (250 μm thick) were introduced into a convection oven and the assembly was heated to 160 °C for 15 min to provide a tight seal of PC-to-PC. The cross-sectional view of the multiple channels represents a permanent tight-seal as well as a minimized microstructure deformation of the channel architecture (see picture (B4) in Figure 2).

2.2 Extraction of DNA from cell lines

Genomic DNA was extracted from cell lines of known K-*ras* genotype (HT29, wild-type; SW1116, G12A; LS180, G12D; SW620, G12V; DLD1, G13D) [18]. Cell lines were grown in RPMI culture media with 10% bovine serum. Harvested cells ($\sim 1 \times 10^7$) were resuspended in DNA extraction buffer (10 mM Tris-HCl, pH 7.5, 150 mM NaCl, 2 mM EDTA, pH 8.0) containing 0.5% SDS and 200 μg/mL proteinase K and incubated at 37 °C for 4 h. Thirty percent (v/v) of 6 M NaCl was added to the mixture, and the samples were centrifuged. DNA was precipitated from the supernatant with three volumes of EtOH, washed with 70% EtOH, and resuspended in TE buffer (10 mM Tris-HCl, pH 7.2, 2 mM EDTA, pH 8.0).

2.3 PCR and LDR conditions

The PCR cocktail consisted of 10 mM Tris-HCl buffer (pH 8.3) containing 10 mM KCl, 3.0 mM $MgCl_2$, 200 μM dNTPs, 500 nM forward and reverse primers, 10 ng/μL genomic DNA extracted from the cell lines and 0.8 U/μL *Taq* DNA polymerase, Stoffel fragment (Applied Biosystems, Foster City, CA). The primers used were as follows: forward = 5′ TTA AAA GGT ACT GGT GGA GTA TTT GAT A 3′; reverse = 5′ AAA ATG GTC AGA GAA ACC TTT ATC TGT 3′.

The LDR cocktail typically employed in this work consisted of 15 mM Tris-HCl (pH 8.3), 100 mM KCl, 6.5 mM $MgCl_2$, 0.25 mM NAD^+ (nicotinic adenine dinucleotide, a cofactor for ligase enzyme), 0.005% Triton X-100, 100 nM of the discriminating primers, 100 nM fluorescently-labeled common primer (see Table 1 for sequences of primers), 50 vol% PCR products, and 2.5 U/μL of *Taq* DNA ligase enzyme (New England Biolabs, Beverly, MA). The concentration ratio of the mutant-to-wild-type DNA was adjusted from 0:1 (mutant:wild-type, control) to 1:1000. To test the fidelity and yield of the LDR reaction, slab gel electrophoresis was run on an aliquot of each reaction (1 μL LDR product was mixed with 2 μL loading dye and then, 1 μL of that mixture was loaded into an individual well of a polyacrylamide gel).

2.4 Microchip operation

Film resistance heaters (KHLV-101/10, Omega Engineering, Inc., Stamford, CT) were attached to the cover plate of the PCR/LDR microchip. Capillary tubes (75 μm i.d.; 363 μm o.d.; 18 cm long; Polymicro Technologies, Phenix, AZ) were affixed to the chip reservoirs (R1–R3; refer to Figure 3) to aid in loading and picking the processed samples from the chips.

A syringe pump (Pico Plus, Harvard Apparatus, Holliston, MA) was used to drive the PCR and the LDR mixtures at the same volumetric flow rate through the flow-through bioreactor. Glass syringes (Hamilton, Reno, NV) with syringe-to-capillary adapters (InnovaQuartz, Phoenix, AZ) were used to make the low dead volume connections between the pump and the microfluidic chip. The resultant CFPCR product was sequentially mixed with the LDR cocktail via a Y-shaped passive micromixer. Temperatures were maintained during operation using the heaters under closed-loop PID control (CN77R340, Omega Engineeing, Inc., Stamford, CT). Temperature feedback was supplied through Type-K thermocouples (5TC-TT-K-36-36, Omega Engineering, Inc., Stamford, CT) mounted between the cover plates and film heaters. The arrangement of temperature zones on the microchannel (94 °C for denaturing and 60 °C for annealing/extension (PCR) and annealing/ligation (LDR)) is depicted in Figure 3.

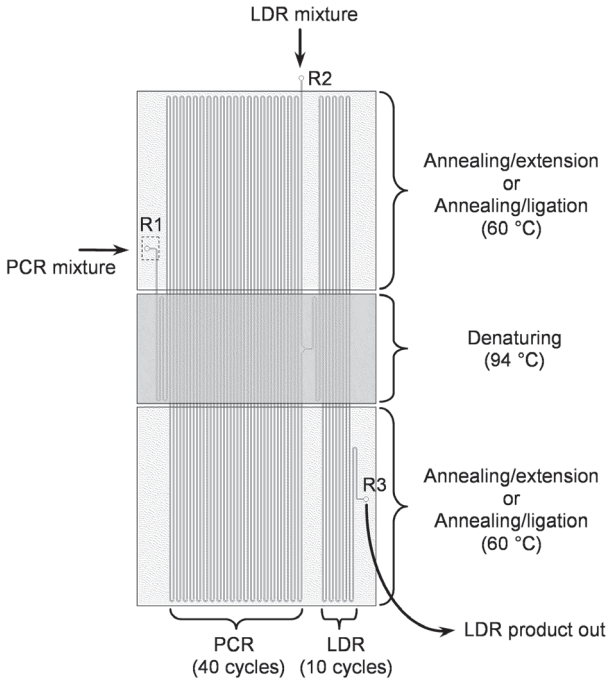

Figure 3: Topographical layout of the CFPCR/CFLDR biochip. Three different Kapton film heaters were attached to the appropriate positions on the CFPCR/CFLDR chip for providing the required isothermal zones. Thermocouples were inserted between the microchip cover plate and the film heaters for monitoring temperatures.

The LDR products were collected from R3 into vials and subjected to gel electrophoresis for analysis. In order to examine the primary PCR results, the PCR products were extracted from R2 (see Figure 3) into vials with R3 sealed. Electrophoresis of PCRs and LDRs was accomplished using either a 3% precast agarose gel (Bio-Rad Laboratories, Hercules, CA) or a 5.5% (w/v) cross-linked polyacrylamide gel (Li-Cor Biotechnology, Lincoln, NE). The agarose gel electrophoresis was conducted at an electric field of

Oligos	Sequences ($5'\rightarrow3'$)	Size (mer)
K-*ras* c12 com-2	p[a]TGGCGTAGGCAAGAGTGCCT-Cy5.5[b]	20
K-*ras* c12.2WtG	**GCTGAGGTCGATGCTGAGGTCGCA**AAACTTGTGGTAGTTGGAGCTGG	47
K-*ras* c12.2D	**GCTGCGATCGATGGTCAGGTGCTG**AAACTTGTGGTAGTTGGAGCTGA	47
K-*ras* c12.2A	**GCTGTACCCGATCGCAAGGTGGTC**AAACTTGTGGTAGTTGGAGCTGC	47
K-*ras* c12.2V	**CGCAAGGTAGGTGCTGTACCCGCA**AAACTTGTGGTAGTTGGA GCTGT	47

[a]p, phosphorylated. [b]Cy5.5, $\lambda_{ex} = 685$ nm; $\lambda_{em} = 706$ nm. The boldface sequences are not complementary to the sequence of the template DNA.

Table 1: Sequences of Oligonucleotides used in the PCR/LDR assays.

7 V/cm for 1 h and post-stained with ethidium bromide for visualizing the electrophoretic bands. The polyacrylamide gel was polymerized between two borofloat glass plates (21 cm × 25 cm) and placed in the Global IR^2 DNA analysis system (Li-Cor Biotechnology, Lincoln, NE). Slab gel electrophoresis was typically run at -1500 V for 2 h. The fluorescence bands were integrated over each separation lane with ImageQuant software (Amersham Biosciences, Piscataway, NJ).

3 Results and discussion

3.1 Effect of presence of *Taq* DNA polymerase on LDR

One of the bottlenecks for carrying out different biological reactions sequentially is that carryover from the primary reaction may interfere with the subsequent reaction, resulting in poor product yield and/or fidelity. Therefore, inactivation, extraction and/or purification of the primary reaction products are usually required before those products are incorporated into the next processing step. It is known that *Taq* DNA polymerase, which is the most commonly used polymerase for PCR amplification, has an inherent $5'\rightarrow3'$ exonuclease activity, which cleaves the $5'$-terminus of double-stranded DNA releasing free nucleotides [12]. Therefore, the use of *Taq* in the PCR phase may lead to cleavage of the common primer by the PCR forward and/or the discriminating primers due to the $5'\rightarrow3'$ exonuclease activity in the LDR phase, reducing the successful ligation between the $3'$-terminus of the discriminating primer and the $5'$-terminus of the adjacent common primer (refer to Figure 4(A)). In addition, the discriminating primer can internally hybridize to the primary PCR products, which can itself undergo a PCR amplification even in the LDR phase (i.e. generation of 200 bp nested PCR product depicted in Figure 4(A)), also reducing the LDR product amount. To alleviate the reduction in LDR product amount and the generation of artifacts by the carryover *Taq*, a post-PCR treatment with proteinase K has conventionally been employed in order to deactivate this enzyme prior to LDR [2,5,18]. Unfortunately, the incorporation of a *Taq* inactivation step following PCR and prior to the LDR would make the system design more complicated and microfluidic manipulation more difficult due to the long incubation time required for complete *Taq* inactivation ($\sim$ 2 h). Also, removal of the proteinase K would be required prior to LDR to prevent inactivation of the ligation enzyme.

One of the simplest ways for minimizing any inhibitory associated with the carryover polymerase is to use *Taq* DNA polymerase Stoffel fragment, which lacks $5'\rightarrow3'$ exonuclease activity, instead of using the conventional *Taq* polymerase in the primary PCR phase. We therefore investigated the effects of Stoffel fragment incorporation on LDR in terms of product yield and ligation fidelity in order to determine if even Stoffel fragment essentially needs to be completely inactivated before being incorporated into the LDR phase. Coupled PCR/LDR processings were carried out under different conditions as summarized in Table 2 and the resultant LDR products were analyzed by both agarose gel electrophoresis and polyacrylamide gel electrophoresis (Figure 4(B)). A low resolution 3% agarose gel was used for analyzing the products to size the potential PCR amplicons produced. On the other hand, high resolution polyacrylamide gel electrophoresis of the PCR/LDR product solutions was employed for interrogating the LDR products.

Briefly, PCR amplifications were performed using the microfluidic reactor in the presence of Stoffel fragment, and for samples #1 and 2, the PCR product solutions were collected from the end of microchannel (R2) into vials and treated with proteinase K at 65 °C for 30 min to inactivate Stoffel fragment followed by inactivation of the leftover proteinase K at 90 °C for 15 min using an off-chip incubator and then mixed with the LDR cocktail, being introduced form R2 to the reactor and subjected to CFLDR (used as the reference, no polymerase activity), while for samples #3 and 4, the PCR product solutions obtained with the CFPCR were directly incorporated into the LDR-cycling phase without any pre-treatment. All difference between samples #1 and 2 (or between samples #3 and 4) was the discriminating primers employed, that is cZip1-K-*ras* c12.2WtG for samples #1 and 3 (positive control LDR), a mixture of cZip-K-*ras* c12.2D, A and V for samples #2 and 4 (negative control LDR). The polyacrylamide gel electrophoresis results (lower panel in Figure 4(B))

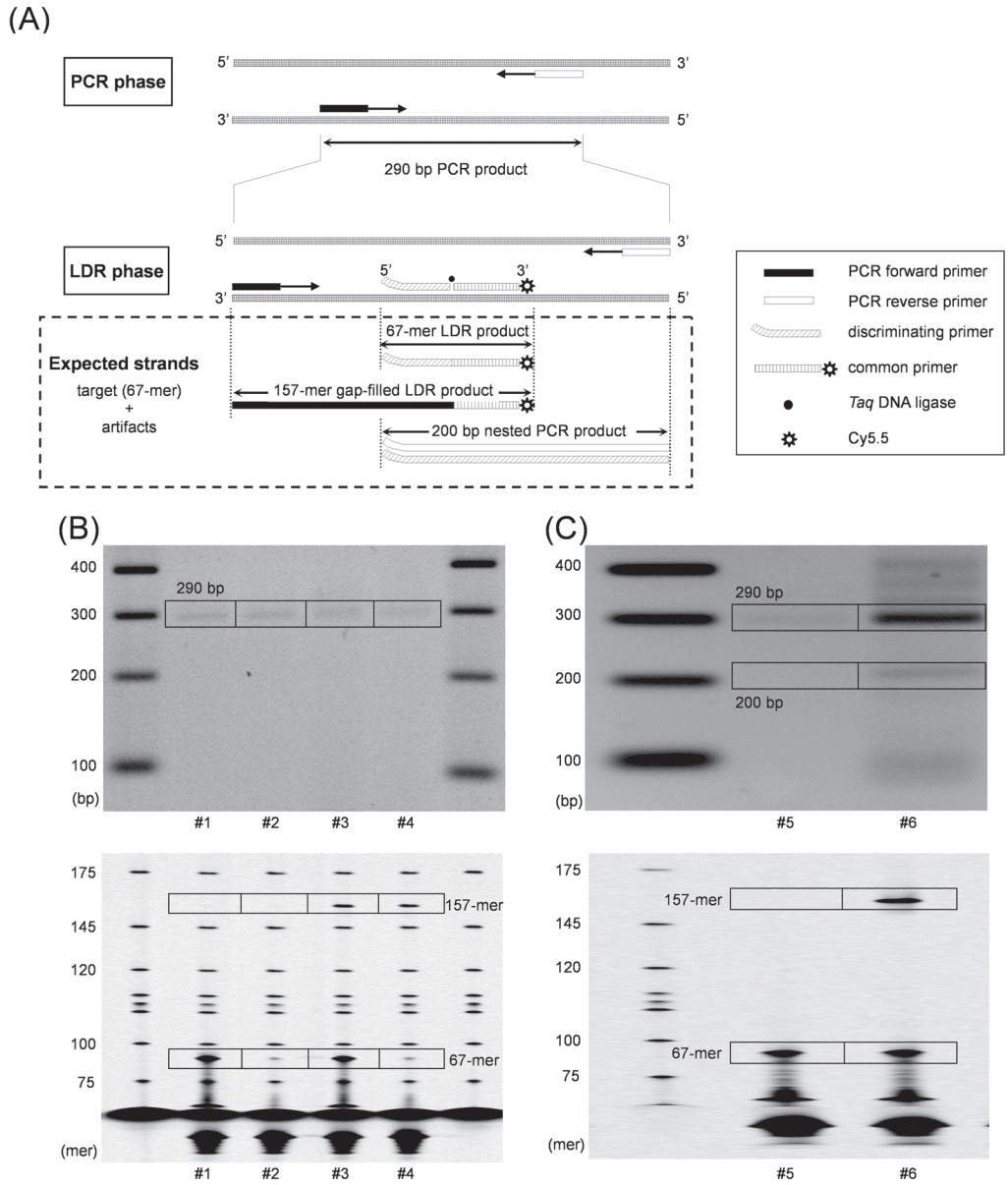

Figure 4: Effects of carryover *Taq* DNA polymerase on LDR. (A) Schematic representation of sequential PCR/LDR reactions and the amplification products. (B) Agarose gel electrophoresis (upper panel) and polyacrylamide gel electrophoresis (lower panel) of the PCR/LDR products obtained by the microfluidic device. (C) The same electrophoresis experiments as those in (B) except that the PCR/LDR products were obtained by a commercial thermal cycler. See Table 2 for the detailed experimental conditions.

showed that the LDR with active Stoffel fragment did not differ in product yield and ligation fidelity from the LDR in the presence of inactivated Stoffel fragment. For example, sample #3, where LDR was carried out in the presence of active polymerase, showed the product amount of $90 \pm 18\%$ as compared with that for sample #1. A major difference appeared in the results between the presence and the absence of active polymerase in the LDR phase was that the incorporated active polymerase produced some additional artifacts in the LDR-cycling phase. For example, the carryover PCR forward primer can elongate towards the LDR primers due to the active polymerase, and the $3'$-terminus of the extending PCR primer can be ligated with the phospholylated $5'$-end of the common primer (referred to as "gap-filling" ligation) [1], producing the 157-mer LDR product (see samples #3 and 4 in the lower panel in Figure 4(B)). The amount of the 157-mer LDR product was reasonably independent of the nature of the nucleotide

Sample	Post-PCR treatment[a]	LDR		Thermal cycler	Cycle number	
		Control[b]	Discriminating primer[c]		PCR	LDR
#1	+	Pos.	G	Microfluidic device	40	10
#2	+	Neg.	D+A+V	Microfluidic device	40	10
#3	−	Pos.	G	Microfluidic device	40	10
#4	−	Neg.	D+A+V	Microfluidic device	40	10
#5	+	Pos.	G	Commercial machine	30	30
#6	−	Pos.	G	Commercial machine	30	30

[a](+), 20 μL of PCR product was incubated with 1.6 μL of proteinase K at 65 °C for 30 min followed by thermal inactivation at 90 °C for 15 min. (−), Any pre-treatment was not performed.
[b]Wild-type template was used for the positive and negative control experiments.
[c]G, K-*ras* c12.2WtG; D, K-*ras* c12.2D; A, K-*ras* c12.2A; V, K-*ras* c12.2V (refer to Table 1).

Table 2: Summarized experimental procedures used to test the coupled PCR/LDR.

(allelic composition) at 3′-end of the discriminating primer because 157-mer artifacts are the products formed from the PCR primer and the common primer (refer to Figure 4(A)). However, the amount of the 67-mer target strand highly depends on the allelic composition at 3′-end of the discriminating primer, and hence enabling the selective detection of the point mutations at the specific allele. As for sample #3, the amount of 157-mer LDR product was ca. 3-fold lower than that of 67-mer target product, which was probably because the gap-filling process fell behind ligation process between the discriminating primer and the common primer due to the lower melting temperature of the PCR forward primer than that of the discriminating primer. It should be noted that a gap-filled LDR product can never be formed with the PCR forward primer and the discriminating primer since the 5′-end of the discriminating primer is not phosphorylated.

A bench-top experiments using a commercial thermal cycler with an increased LDR cycling number (30 cycles) revealed that PCR amplification can proceed even in the subsequent LDR-cycling phase due to the carryover active polymerase, which clearly appeared in the agarose gel electrophoresis results shown in Figure 4(C) with the following two points: (1) the increased amount of the target PCR product (290 bp); (2) the generation of the secondary PCR products (i.e. 200 bp nested amplicon) which are the extension products formed with the discriminating primers and the PCR reverse primers (compare lane #6 with #5 in the upper panel). It should be noted that the labeled dye at the 3′-end of the common primer prevents the primer from extending toward 3′ direction and hence no nested PCR product is formed along with the PCR reverse primer.

3.2 CFPCR/CFLDR using the microfluidic device

A lack of degradation of LDR yields and fidelity from PCR product solutions that were not deactivated allowed us to design a simple flow-through microfluidic reactor containing PCR and LDR processing steps in sequence and employing a Y-shaped passive diffusional micromixer to allow mixing the PCR mix with the LDR reagents prior to thermal cycling for the LDR. This mixer type has been investigated experimentally and numerically with a simplified three- or two-dimensional model [11,13,14, 15,28,31]. Some groups performed theoretical studies of convective/diffusive transport of solutes from two tributaries in the main channel as a function of the Peclet number and the normalized channel dimensions [11,31]. We have applied the dimensionless analysis proposed by Wu et al. [31] to the present study to roughly estimate a mixing length for the macromolecules such as the DNA ligase and the PCR products under the particular conditions employed in the present study.

The two-dimensional model of a passive micromixer with two inlet streams is schematically represented in Figure 5(A). Briefly, the two streams merge into a single channel with the width of W. One stream is the solute with a concentration of c_0, the other stream is the solvent with a concentration of $c = 0$. The solute flow in the channel is assumed to have a constant velocity of u. The transport equation for both diffusive and convective effects can be formulated as

$$D\left(\frac{\partial^2 c}{\partial x^2} + \frac{\partial^2 c}{\partial y^2}\right) = u\frac{\partial c}{\partial x}, \tag{1}$$

where D is the diffusion coefficient of the species. By introducing the dimensionless variables into the coordinate system $x^* = x/W$, $y^* = y/W$, the dimensionless concentration $c^* = c/c_0 - 1/2$ and the Peclet number

$$Pe = \frac{uW}{D}, \tag{2}$$

equation (1) can be formulated in the dimensionless form as

$$\left(\frac{\partial^2 c^*}{\partial x^{*2}} + \frac{\partial^2 c^*}{\partial y^{*2}}\right) = Pe\frac{\partial c^*}{\partial x^*}. \tag{3}$$

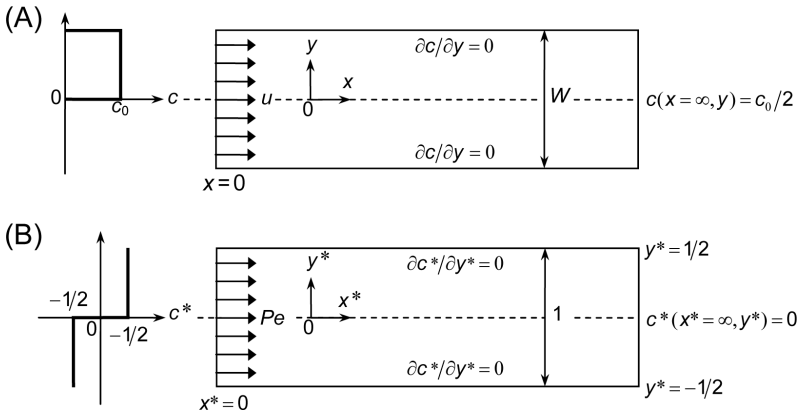

Figure 5: Schematic representation of the two-dimensional model for the micromixer: (A) the actual model and (B) the dimensionless model. In the model of (A), a diffusive mixer with two inlet channels (each $W/2$wide) that feed into a single channel with a width of W. Up the left-most inlet channel solution at an initial concentration of c_0 is flowed at a constant velocity of u, while down the other inlet water is flowed at the same velocity of u. Streamwise and spanwise distances from the origin (i.e. junction of the two inlet channels) are defined as x and y, respectively. In the model of (B), the variables of c, u, x and y were replaced with dimensionless variables of $c^*(= c/c_0 - 1/2)$, Pe $(= uW/D)$, $x^*(= x/W)$ and $y^*(= y/W)$, respectively.

The model for (3) is depicted in Figure 5(B). The boundary conditions for (3) are

$$\begin{aligned} c^*|_{(x^*=0,\ 0<y^*<1/2)} &= 1/2 \\ c^*|_{(x^*=0,\ -1/2<y^*<0)} &= -1/2 \\ c^*|_{(x^*=\infty)} &= 0. \end{aligned} \tag{4}$$

Since the channel wall is impermeable, the boundary condition for the zero flux at the channel walls is

$$\left.\frac{\partial c^*}{\partial y^*}\right|_{(y=\pm 1/2)} = 0. \tag{5}$$

For larger Peclet numbers, the diffusive term in the x^*-direction is much smaller than the convective term in (3). Thus, (3) can be simplified as

$$\frac{\partial^2 c^*}{\partial {y^*}^2} = Pe\frac{\partial c^*}{\partial x^*}. \tag{6}$$

The solution of (6) with the boundary conditions of (4) and (5) is

$$\begin{aligned} c^*\left(x^*, y^*\right) = \frac{1}{\pi}\sum_{n=1}^{\infty} \exp\left[\frac{-\pi^2(2n-1)^2 x^*}{Pe}\right] \\ \times \sin\left[\pi(2n-1)y^*\right]\frac{1-\cos\left[\pi(2n-1)\right]}{2n-1}. \end{aligned} \tag{7}$$

Concentration variations obtained from two-dimensional simulations are shown in Figure 6. It is clear that a short mixing length requires a small Peclet number, which corresponds to a slow velocity u, a small channel width W or a large diffusion coefficient D. A diffusion coefficient for a small molecule with its molecular weight of several hundreds (e.g. fluorescent dyes) is on the order of $10^{-10}\,\mathrm{m^2\,s^{-1}}$ in a typical aqueous solution [24]. Thus, the Peclet number for these molecules is on the order of $Pe = 10^3$ with the

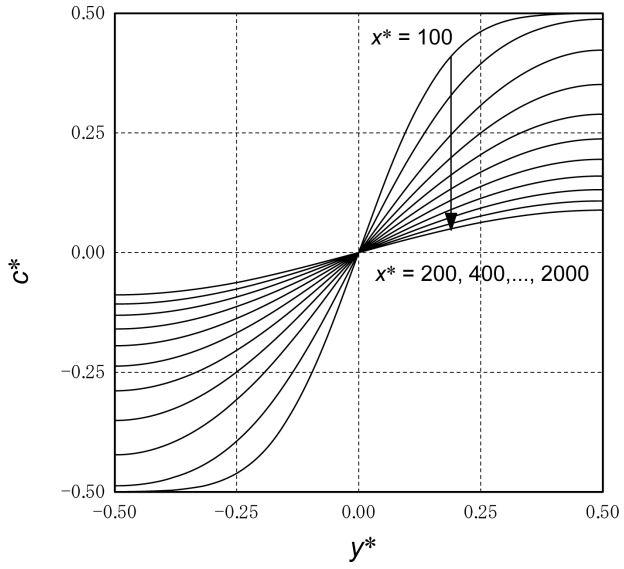

Figure 6: Concentration distribution across the microchannel simulated with the dimensionless model. The distributions of the dimensionless concentration (c^*) in the spanwise direction are represented at the various streamwise distances (x^*) of 100–2000 (i.e. 1–20 cm with the given channel width of 100 μm) assuming a relatively large Peclet number of ca. 10^4 for the macromolecules ($D = 3 \times 10^{-10}\,\mathrm{m^2\,s^{-1}}$) with the applied flow velocity of $2.67\,\mathrm{mm\,s^{-1}}$.

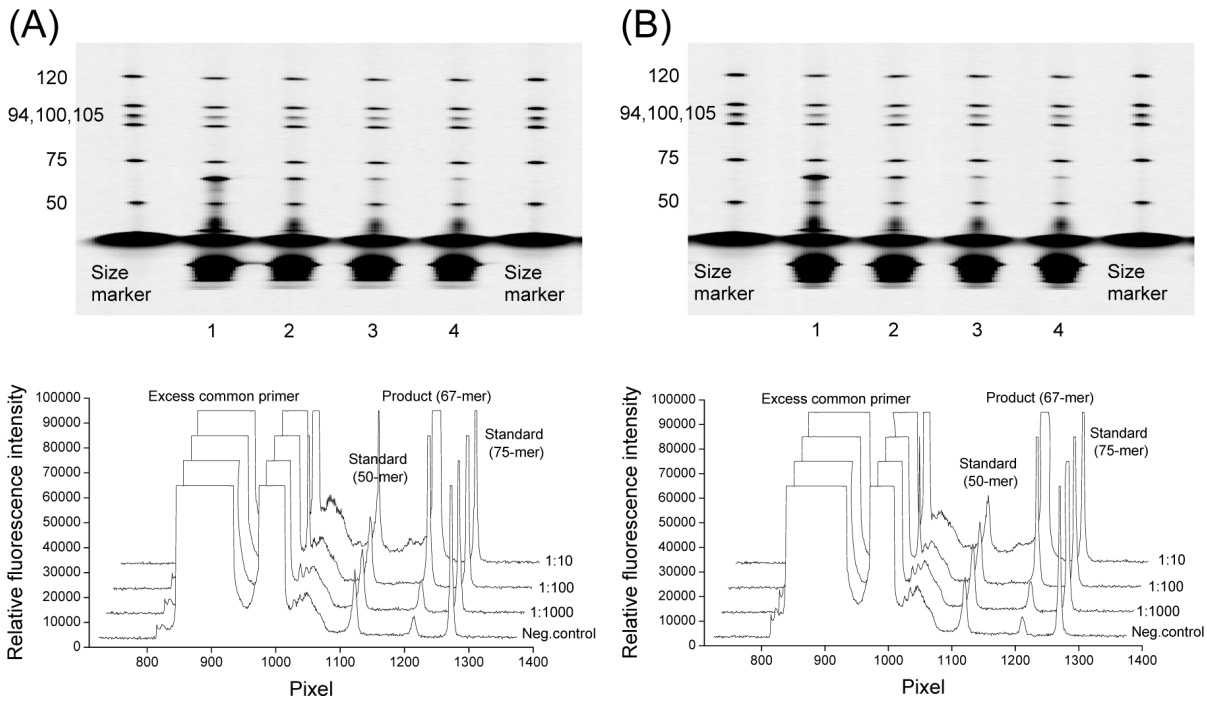

Figure 7: Mutational analysis of point mutations in K-*ras* in the presence of wild-type and mutant sequences and wild-type sequence only (control). The PCR products were treated with proteinase K prior to CFLDR for (A) while the products were online incorporated into the CFLDR for (B). The LDR products were mixed with size markers (50, 75, 94, 100, 105 and 120-mer) prior to loading onto the gel matrix, and then electrophoretically sorted using a 5.5% polyacrylamide gel matrix (upper panel). Fluorescence was integrated over the individual lanes (lower panel).

given flow velocity of $2.67\,\mathrm{mm\,s^{-1}}$ and the channel width of $100\,\mu$m in the present study. On the other hand, the diffusion coefficients for the giant molecules employed in this work such as *Taq* DNA ligase (ca. $80\,$kDa) and $290\,$bp PCR product (ca. $190\,$kDa) are approximately an order larger than those for the small molecules [13, 23], which results in an order larger Peclet number of ca. 10^4. According to the simulation shown in Figure 6, the macromolecules requires a rather large mixing length of $x^* = 2000$ (i.e. $x = 20\,\mathrm{cm}$) until they fully disperse in the spanwise direction. However, it should be noted that the LDR could proceed prior to the uniform distribution of the macromolecules in the spanwise direction of the microchannel. In addition, the total channel length of $50\,$cm for the LDR processing can compensate for the long mixing length. In fact, amounts of the final products obtained with this reactor were large enough for the fluorescence visualization.

We next examined fluorescence signals generated from correct ligation with the mutant template and backgrounds generated from mismatched ligations occurring from the wild-type template. Mixtures of wild-type and mutant genomic DNA were PCR amplified by CFPCR with the concentration ratio from 0:1 (mutant:wild-type, control) to 1:1000 using fixed total input DNA amounts ($10\,$ng/L) and the resultant PCR products were online mixed with the LDR mixtures via the Y-shaped mixer, then being subjected to CFLDR cycles. Figure 7 represents CFPCR/CFLDR results when the CFPCR products were either treated with proteinase K prior to CFLDR (A) or online incorporated directly into the CFLDR (B), showing LDR fidelities with the specific discriminating primers (cZip11-K-*ras* c12.2V, see Table 1), which can selectively detect mutations in G12V locus. When only the wild-type alleles were present in the LDR mixture, small amounts of mismatched products were generated (i.e. background noise in LDR assay) as shown in lane 4, which is due to the ability of the thermostable ligase to rapidly dissociate from substrate containing mismatches. The mutation signal (matched ligation product) was distinguished from noise (mismatched ligation product) at a sensitivity level of 1:1000 (compare lane 3 with 4), allowing for the potential of high sensitivity discrimination of the target mutations from the noise due to the false ligation. It seems that whether the incorporated Stoffel fragment is inactivated or not, it renders no influence on the discrimination capability (compare the result in (A) with that in (B)). Since the flows of the PCR product and the LDR mixture were driven at the same volumetric flow rate ($0.8\,\mu$L/min), the combined flow rate at the mixing junction provided a composite flow rate of $1.6\,\mu$L/min for the LDR thermal cycling. Hence, a 10-cycles LDR was complete

in ca. 3.1 min with a cycling rate of 18.8 s/cycle (3.8 s for denaturation and 15 s for annealing and ligation).

4 Conclusion

We have microfabricated a flow-through bioreactor, which can rapidly execute sequential CFPCR/CFLDR, for the detection of low-abundant DNA mutatios in gene fragments (K-*ras*) that carry point mutations with high diagnostic value for colorectal cancers. Our experiments indicated the ability to detect one mutant sequence in 1000 normal sequences directly from a mixed population of genomic DNA using the microfluidic reactor. We chose *Taq* polymerase Stoffel fragment, which lacks $5'\rightarrow3'$ exonuclease activity, as a DNA polymerase and investigated how the direct incorporation of the contents in the primary PCR mixture affected the secondary LDR step. Our empirical results showed that the use of Stoffel fragment in the primary PCR phase produced some artifacts in the LDR phase but did not require the post-PCR polymerase inactivation in terms of LDR product yield and mutant discrimination fidelity, which led us to be able to employ the online incorporation of the resultant PCR products directly into the LDR mixture with the simple Y-shaped mixer. The large mixing length estimated by the dimensionless simulation for the macromolecules contained in the reaction fluids was compensated by the prolonged microchannel for the LDR (0.50 m). The miniaturized reaction channel and the continuous-flow operation of the PCR/LDR microthermal cycler accelerated the reaction primarily through its enhanced thermal management capabilities. Because of these attributes, the sequential reactions could be carried out rapidly: 25.0 min for 40 rounds PCR and 3.1 min for 10 rounds LDR ($\sim$ 28.1 min in total). This is a significant reduction in processing time when compared to previous work, where all of these steps were carried out using conventional instrument platforms: 145 min for PCR, 25 min for DNA polymerase inactivation, 95 min for LDR (total processing time $\sim$ 265 min) [6].

Acknowledgments The authors thank the National Institutes of Health (National Institute of Bioengineering and BioImaging, EB002115), the National Science Foundation under Grant EPS-0346411 and the State of Louisiana Board of Reagents for financial support of this work.

References

[1] K. Abravaya, J. J. Carrino, S. Muldoon, and H. H. Lee, *Detection of point mutations with a modified ligase chain reaction (Gap-LCR)*, Nucleic Acids Res, 23 (1995), 675–682.

[2] F. Barany, *Genetic disease detection and DNA amplification using cloned thermostable ligase*, Proc Natl Acad Sci U S A, 88 (1991), 189–193.

[3] M. A. Burns, C. H. Mastrangelo, T. S. Sammarco, F. P. Man, J. R. Webster, B. N. Johnsons, et al., *Microfabricated structures for integrated DNA analysis*, Proc Natl Acad Sci U S A, 93 (1996), 5556–5561.

[4] Y. W. Cheng, C. Shawber, D. Notterman, P. Paty, and F. Barany, *Multiplexed profiling of candidate genes for CpG island methylation status using a flexible PCR/LDR/Universal Array assay*, Genome Res, 16 (2006), 282–289.

[5] R. Favis, J. P. Day, N. P. Gerry, C. Phelan, S. Narod, and F. Barany, *Universal DNA array detection of small insertions and deletions in BRCA1 and BRCA2*, Nat Biotechnol, 18 (2000), 561–564.

[6] N. P. Gerry, N. E. Witowski, J. Day, R. P. Hammer, G. Barany, and F. Barany, *Universal DNA microarray method for multiplex detection of low abundance point mutations*, J Mol Biol, 292 (1999), 251–262.

[7] M. Hashimoto, F. Barany, and S. A. Soper, *Polymerase chain reaction/ligase detection reaction/hybridization assays using flow-through microfluidic devices for the detection of low-abundant DNA point mutations*, Biosens Bioelectron, 21 (2006), 1915–1923.

[8] M. Hashimoto, F. Barany, F. Xu, and S. A. Soper, *Serial processing of biological reactions using flow-through microfluidic devices: coupled PCR/LDR for the detection of low-abundant DNA point mutations*, Analyst, 132 (2007), 913–921.

[9] M. Hashimoto, P. C. Chen, M. W. Mitchell, D. E. Nikitopoulos, S. A. Soper, and M. C. Murphy, *Rapid PCR in a continuous flow device*, Lab Chip, 4 (2004), 638–645.

[10] M. Hashimoto, M. L. Hupert, M. C. Murphy, S. A. Soper, Y. W. Cheng, and F. Barany, *Ligase detection reaction/hybridization assays using three-dimensional microfluidic networks for the detection of low-abundant DNA point mutations*, Anal Chem, 77 (2005), 3243–3255.

[11] M. A. Holden, S. Kumar, E. T. Castellana, A. Beskok, and P. S. Cremer, *Generating fixed concentration arrays in a microfluidic device*, Sens Actuators B Chem, 92 (2003), 199–207.

[12] P. M. Holland, R. D. Abramson, R. Watson, and D. H. Gelfand, *Detection of specific polymerase chain reaction product by utilizing the $5'\rightarrow3'$ exonuclease activity of Thermus aquaticus DNA polymerase*, Proc Natl Acad Sci U S A, 88 (1991), 7276–7280.

[13] A. E. Kamholz, E. A. Schilling, and P. Yager, *Optical measurement of transverse molecular diffusion in a microchannel*, Biophys J, 80 (2001), 1967–1972.

[14] A. E. Kamholz, B. H. Weigl, B. A. Finlayson, and P. Yager, *Quantitative analysis of molecular interaction in a microfluidic channel: the T-sensor*, Anal Chem, 71 (1999), 5340–5347.

[15] A. E. Kamholz and P. Yager, *Theoretical analysis of molecular diffusion in pressure-driven laminar flow in microfluidic channels*, Biophys J, 80 (2001), 155–160.

[16] J. Khandurina, T. E. McKnight, S. C. Jacobson, L. C. Waters, R. S. Foote, and J. M. Ramsey, *Integrated system for rapid PCR-based DNA analysis in microfluidic devices*, Anal Chem, 72 (2000), 2995–3000.

[17] M. Khanna, W. Cao, M. Zirvi, P. Paty, and F. Barany, *Ligase detection reaction for identification of low abundance mutations*, Clin Biochem, 32 (1999), 287–290.

[18] M. Khanna, P. Park, M. Zirvi, W. Cao, A. Picon, J. Day, et al., *Multiplex PCR/LDR for detection of K-ras mutations in primary colon tumors*, Oncogene, 18 (1999), 27–38.

[19] C. G. Koh, W. Tan, M. Q. Zhao, A. J. Ricco, and Z. H. Fan, *Integrating polymerase chain reaction, valving, and electrophoresis in a plastic device for bacterial detection*, Anal Chem, 75 (2003), 4591–4598.

[20] M. U. Kopp, A. J. Mello, and A. Manz, *Chemical amplification: continuous-flow PCR on a chip*, Science, 280 (1998), 1046–1048.

[21] E. T. Lagally, I. Medintz, and R. A. Mathies, *Single-molecule DNA amplification and analysis in an integrated microfluidic device*, Anal Chem, 73 (2001), 565–570.

[22] X. J. Lou, N. J. Panaro, P. Wilding, P. Fortina, and L. J. Kricka, *Mutation detection using ligase chain reaction in passivated silicon-glass microchips and microchip capillary electrophoresis*, Biotechniques, 37 (2004), 392, 394, 396–398.

[23] D. Luo, K. Woodrow-Mumford, N. Belcheva, and W. M. Saltzman, *Controlled DNA delivery systems*, Pharm Res, 16 (1999), 1300–1308.

[24] M. S. Munson, K. R. Hawkins, M. S. Hasenbank, and P. Yager, *Diffusion based analysis in a sheath flow microchannel: the sheath flow T-sensor*, Lab Chip, 5 (2005), 856–862.

[25] P. J. Obeid, T. K. Christopoulos, H. J. Crabtree, and C. J. Backhouse, *Microfabricated device for DNA and RNA amplification by continuous-flow polymerase chain reaction and reverse transcription-polymerase chain reaction with cycle number selection*, Anal Chem, 75 (2003), 288–295.

[26] R. P. Oda, M. A. Strausbauch, A. F. Huhmer, N. Borson, S. R. Jurrens, J. Craighead, et al., *Infrared-mediated thermocycling for ultrafast polymerase chain reaction amplification of DNA*, Anal Chem, 70 (1998), 4361–4368.

[27] C. Situma, Y. Wang, M. Hupert, F. Barany, R. L. McCarley, and S. A. Soper, *Fabrication of DNA microarrays onto poly(methyl methacrylate) with ultraviolet patterning and microfluidics for the detection of low-abundant point mutations*, Anal Biochem, 340 (2005), 123–135.

[28] S. P. Sullivan, B. S. Akpa, S. M. Matthews, A. C. Fisher, L. F. Gladden, and M. L. Johns, *Simulation of miscible diffusive mixing in microchannels*, Sens Actuators B Chem, 123 (2007), 1142–1152.

[29] H. Wang, J. Chen, L. Zhu, H. Shadpour, M. L. Hupert, and S. A. Soper, *Continuous flow thermal cycler microchip for DNA cycle sequencing*, Anal Chem, 78 (2006), 6223–6231.

[30] Y. Wang, B. Vaidya, H. D. Farquar, W. Stryjewski, R. P. Hammer, R. L. McCarley, et al., *Microarrays assembled in microfluidic chips fabricated from poly(methyl methacrylate) for the detection of low-abundant DNA mutations*, Anal Chem, 75 (2003), 1130–1140.

[31] Z. Wu, N.-T. Nguyen, and X. Huang, *Nonlinear diffusive mixing in microchannels: theory and experiments*, J Micromech Microeng, 14 (2004), 604–611.